Macromolecules

Article

pubs.acs.org/Macromolecules

Correlated Diffusivities, Solubilities, and Hydrophobic Interactions in Ternary Polydimethylsiloxane–Water–Tetrahydrofuran Mixtures

Stephen H. Donaldson, Jr.,[†,§] Justin P. Jahnke,[†] Robert J. Messinger,[†] Åsa Östlund,[†] David Uhrig,[‡] Jacob N. Israelachvili,[†] and Bradley F. Chmelka*[,†]

[†]Department of Chemical Engineering, University of California, Santa Barbara, Santa Barbara, California 93106-5080, United States

[‡]Center for Nanophase Materials, Sciences Division, Oak Ridge National Laboratory, P.O. Box 2008, Oak Ridge, Tennessee 37831, United States

[§]Departement de Physique, Ecole Normale Supérieure/PSL Research University, CNRS, 24 rue Lhomond, 75005 Paris, France

Supporting Information

ABSTRACT: Bulk thermodynamic and kinetic properties of mixtures are generally composition dependent, often in complicated ways, especially for partially miscible and multicomponent systems. Combined ^{1}H chemical shift, ^{1}H diffusion NMR, and surface forces analyses establish the compositional dependences of water solubility and self-diffusion in ternary polymeric polydimethylsiloxane–water–tetrahydrofuran (THF) mixtures. The addition of THF significantly increases the solubility of water, while decreasing its diffusivity, in hydrophobic polydimethylsiloxane. Minimum values for the self-diffusivities of both water and THF coincide with a minimum in the hydrophobic adhesion energy between silicone polymer thin films near the same binary composition of 0.20 mole fraction THF. Such interrelated diffusivities, solubilities, and hydrophobic interactions are analyzed with respect to hydrogen bonding among the constituent species to account for the bulk physical properties of technologically important mixtures of silicone polymers with water and/or cosolvents.

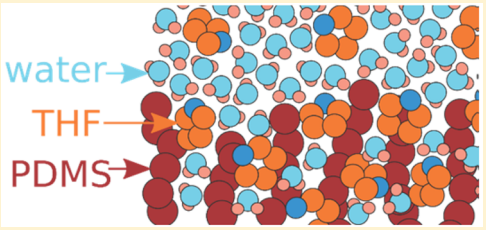

INTRODUCTION

Polymers are often processed from or otherwise in contact with multicomponent solutions, in which macromolecular and solvent species interact in complicated ways to influence material structures and functions.[1] However, understanding and correlating the compositional dependences of kinetic properties, such as diffusivities or other rate-dependent processes, with thermodynamic quantities, such as solubilities and interaction energies, are challenging, especially in complicated mixtures. In the absence of concentration and thermal gradients, the Brownian diffusivities of molecules and particles are governed by the Stokes–Einstein relation,[2] which describes competition between thermal motions and frictional drag in a viscous medium. Even at thermodynamic equilibrium, the transient structures of liquids are governed by molecules undergoing random thermal motions, molecular collisions, and interactions that influence their mean-free paths and self-diffusion properties.

In hydrogen-bonding liquids, such as water, molecular liquid structures can be described in terms of interplay between self-diffusion and the kinetics of hydrogen (H)-bond formation and breaking.[3] Measurements of self-diffusion generally occur over relatively long length and time scales, for which a liquid can be considered to be at thermodynamic equilibrium, and depend on molecular size and solute–solvent interactions. In multicomponent mixtures, self-diffusivities reflect time-averaged association states among the molecular species and, thus, are highly dependent on the concentration and physicochemical properties of each component. Amphiphilic molecules and mixtures of polar and nonpolar species are even more complicated due to the diverse intermolecular interactions that govern their macroscopic properties, including their often low mutual solubilities. Mixtures of polymers and small molecules present additional complexities, such as macromolecular entanglements or tortuosity, that may limit the mean free paths of diffusing species. This includes the silicone polymer–water–tetrahydrofuran (THF) system, which exhibits kinetic and thermodynamic properties that are difficult to attribute solely to those of their individual constituent species or to their binary mixtures. For example, whereas binary water–THF and THF–polydimethylsiloxane mixtures are miscible under ambient conditions, water and hydrophobic polydimethylsiloxane phase-separate.

The physical interactions among THF, water, and polydimethylsiloxane (PDMS, a silicone polymer) are determining factors in their interrelated solubility and diffusion properties. The absence of significant H-bonding and the corresponding increased range and magnitude of hydrophobic interactions lead to bulk phase separation between oil (including hydrophobic PDMS) and water.[4] As depicted schematically in Figure

Received: July 14, 2016
Revised: August 23, 2016
Published: September 12, 2016

DOI: 10.1021/acs.macromol.6b01514
Macromolecules 2016, 49, 6910–6917

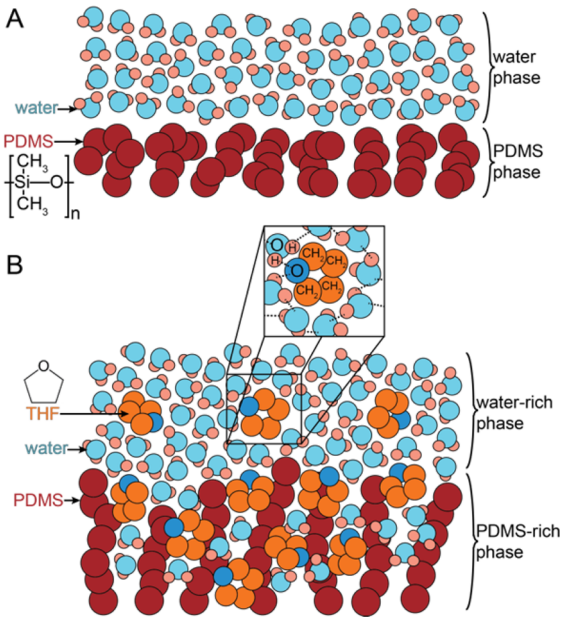

Figure 1. Schematic diagram depicting the behavior of water molecules near PDMS surfaces for (A) pure water and (B) a water−THF mixture. In the presence of water only, the PDMS chains are collapsed, with an adjacent water layer that is unstructured and exhibits diminished hydrogen-bonding near the PDMS surface. In the presence of water and THF, both species can penetrate the PDMS surface, causing the chains to swell.

1A, in the presence of water only, significant H-bonding is not expected between water molecules and hydrophobic PDMS interfaces, leading to phase separation. Conversely, in the presence of the cosolvent THF, water and THF form H-bonds through the lone electron pairs of the THF oxygen atoms (Figure 1B), so that water, THF, and PDMS can form stable ternary solutions. The objective of this study is to understand the molecular-level interactions that influence the macroscopic solubility and diffusivity behaviors of component species in complicated polydimethylsiloxane−water−tetrahydrofuran mixtures. Here, surface forces measurements demonstrate the effects of cosolvents on hydrophobic interactions, which are correlated with ^{1}H chemical shifts that probe local water hydrogen-bonding environments and ^{1}H diffusion NMR measurements that quantify the associated bulk liquid transport properties. These complementary analyses establish that THF affects hydrogen bonding in the ternary mixture, suppressing the interactions that lead to phase separation.

EXPERIMENTAL METHODS

Perdeuterated liquid-state *d*-PDMS was prepared following a modified methodology of Beltzung et al.,[5] resulting in a molecular weight of 25 000 g/mol (degree of polymerization $n \approx 340$) with a polydispersity of 1.1. Perdeuterated hexamethylcyclotrisiloxane (D3-d_{18}) was synthesized in four steps from CD_3I, according to an adapted method of Beltzung and co-workers.[5] In our case, a final fractional distillation of mixed cyclosiloxane product yielded a mixture of D3-d_{18} (majority) and D4-d_{24} (i.e., octamethylcyclotetrasiloxane, minority), taken as a solution in mixed aromatic solvents (benzene, toluene, and xylene). This solution of mixed *d*-monomers was treated chemically with (1) CaH_2 and (2) oligostyryllithium and (3) distilled under vacuum and distributed into ampules. Perdeuterated polydimethylsiloxane (*d*-PDMS) was obtained by polymerizing this monomer anionically, following an adapted method of Bellas and co-workers.[6] The *d*-PDMS was analyzed by size exclusion chromatography using a Polymer Laboratories GPC-50 HPLC instrument equipped with three PLgel 5u mixed-C columns (300 × 7.5 mm) in series, a dual angle light-scattering detector, and a refractive index detector; toluene was used as the mobile phase at a flow rate of 1 mL/min.

Sylgard 184, a common commercial elastomer kit, was purchased from Ellsworth Adhesives and used as-received to prepare the cross-linked PDMS. All water used in these experiments was purified using a Millipore filter to ensure high purity. Undeuterated tetrahydrofuran (THF) was purchased from Sigma-Aldrich (anhydrous, >99.9%) and dried over molecular sieves before use. In some experiments, it was necessary to use deuterated THF or deuterated water (both from Cambridge Isotope Laboratories) to either provide a deuterium lock or enable the observation of dilute species. All *d*-THF and D_2O were used as-received.

Mixtures of the un-cross-linked *d*-PDMS with THF and water were prepared directly in NMR tubes to minimize losses of the valuable perdeuterated *d*-PDMS. Before any mixture was prepared, the un-cross-linked PDMS was dried in a rotary evaporator until all volatiles were removed. Then the desired amount of solvent was added to the NMR tube, and each sample was mixed for several minutes, after which it was allowed to equilibrate for at least 24 h before measurements were conducted. Subsequent measurements were conducted by adding solvent to achieve mixtures with different concentrations of THF or water. When measuring the single-component diffusion of THF in PDMS, in some cases THF was removed after the measurements by using a rotary evaporator to achieve other desired compositions. In all cases where the mixture composition was changed, at least 24 h was allowed for equilibration of the sample before any measurements were conducted.

To prepare cross-linked samples, a Sylgard 184 PDMS mixture was prepared with a 1:10 ratio of curing-to-base components and then immediately mixed with THF in an NMR tube. The sample was then heated at 50 °C for several hours until gelled. Because of the high volatility of the THF, the sample was weighed before and after cross-linking to determine mass-loss during the cross-linking process. This mass loss was entirely attributed to evaporation of volatile THF when calculating the final sample concentrations.

To prepare a PDMS−water mixture that was fully saturated with water, an excess of water was mixed with un-cross-linked PDMS, and the mixture was subsequently allowed to equilibrate for several days. After equilibration, the PDMS−water mixture was centrifuged at 35 000 rpm for 1 h to separate the excess water. The water-saturated PDMS was then transferred to an NMR tube for the NMR measurements.

All of the NMR measurements were performed at 20 °C on a Varian VNMRS 600 MHz spectrometer equipped with a double-resonance probehead (^{1}H−^{19}F/^{15}N−^{31}P 5 mm PFG AutoX DB) capable of gradient strengths up to 73 G/cm with a Performa IV PFG Module gradient amplifier. The single-pulse ^{1}H spectrum was obtained by using a standard 1D pulse sequence with a 11.3 μs 90° pulse, 10 s recycle delay, and 64 scans. The ^{1}H diffusion NMR measurements were conducted using the "one-shot" sequence, as described in detail by Pelta et al.[7] The "one-shot" sequence is similar to the standard Stejskal and Tanner pulse sequence,[8] in which gradient pulses are applied to encode and decode spatial information during a stimulated echo experiment.

Signal attenuation (which results from random diffusion of the molecules away from their initial positions in the sample) during a time delay was measured while systematically incrementing the gradient magnitude G at fixed gradient pulse length δ and diffusion time Δ. Because it is performed as a constant-time experiment, the decay was determined by diffusion only and was not influenced by relaxation effects. For well-resolved NMR signals, this allowed the diffusion coefficient D to be determined. In a normal one-shot experiment, the gradient strength G was incremented logarithmically in 20 steps from about 1−40 G/cm, and each step consisted of 64 scans with a 10 s recycle delay, with constant diffusion time Δ and gradient pulse length δ. The diffusion time Δ was optimized before each series of measurements, so that the signal intensity decayed to about 10−20% of its initial value, and the measured signal intensities

DOI: 10.1021/acs.macromol.6b01514
Macromolecules 2016, 49, 6910−6917

were correlated with the intensity decays to obtain the respective self-diffusion values D.

The surface force measurements used PDMS thin films on gold, which were prepared as described previously,[9,10] or on mica surfaces. For the latter, PDMS films were synthesized by first activating the mica surfaces in a UV/ozone plasma oven (UVOCS Inc. Model T10X10/OES, Montgomeryville, PA) for 30 min to convert surface siloxanes to reactive silanols. The mica surface was then immediately immersed in a 1 vol % solution of (3-trimethoxysilylpropyl)diethylenetriamine (DETAS, Gelest Inc., Morrisville, PA) in methyl ethyl ketone (MEK, Sigma-Aldrich) to obtain approximately a silane monolayer that exposed terminal amine groups. The silane was deposited for 2 h, at which point the surface was immediately rinsed with ethanol, blown dry with N_2, and placed in pure monoglycidyl ether-terminated PDMS liquid (M_n = 5000 g/mol, Sigma-Aldrich). Next, the surface was placed into a vacuum oven at 80 °C for approximately 60 h. The vacuum oven was filled with argon gas to remove oxygen from the environment to prevent oxidation of the back-silvered mica. After the reaction, the fresh PDMS-functionalized mica surfaces were washed using the same procedure described previously,[9] with shorter sonication steps. One second of sonication was used to remove physically bound PDMS molecules without damaging the underlying mica surface.

Surface force measurements were performed at 21 °C with the SFA 2000 (Surforce LLC, Santa Barbara, CA), as described previously.[11] Briefly, PDMS films on gold and back-silvered mica were prepared on cylindrical disks following the procedure described above. The PDMS-functionalized surfaces were then installed into the surface forces apparatus (SFA) in a crossed-cylinder geometry. White light was passed normally through the surfaces and directed to a spectrometer to observe the fringes of equal chromatic order (FECO), which allowed for simultaneous measurements of separation distance and contact mechanics between the two PDMS films. The gold-deposited and back-silvered mica configuration resulted in a two-layer interferometer, from which distances could be determined, as described previously.[12] The two surfaces were immersed in 1 mM NaCl, pH 3 solution, and approach/separation cycles were conducted by bringing the surfaces toward each other and then pulling them apart at a constant quasi-static rate of ~2 nm/s. One surface rested on a force-measuring spring, which deflected in the presence of a force. From this deflection, the force as a function of distance was obtained.

RESULTS AND DISCUSSION

The binary diffusivities of the three components in PDMS−water, PDMS−THF, and water−THF binary mixtures provide insights into the diffusivities in the more complicated ternary system. Crucially, perdeuteration of the (un-cross-linked) PDMS enables observations of the weak ^{1}H NMR signals from dilute water and THF species, which otherwise would be obscured by the dominant ^{1}H signals from nondeuterated PDMS. All of the ^{1}H chemical shifts and self-diffusion coefficients were measured at 20 °C, so the three-component species were in the liquid state. Because of the low solubility of water in PDMS (~0.001 g of H_2O/g of PDMS, ^{1}H chemical shift 1.76 ppm), the binary self-diffusion coefficient of water was feasible to measure by ^{1}H-pulsed-field-gradient (PFG) NMR only for a saturated water−d-PDMS mixture and found to be 3.0 × 10^{-9} m^2/s. Both the measured solubility and self-diffusion of water in liquid phase d-PDMS correspond closely with previously measured values in PDMS.[13,14] By comparison, the bulk self-diffusion coefficient of pure water (2.0 × 10^{-9} m^2/s at 20 °C)[15] is significantly (40%) lower, consistent with stronger hydrogen bonding in pure H_2O. The higher diffusivity and low water concentration suggest that the water molecules possibly diffuse as single molecules, rather than as H-bonded clusters.[13] The higher measured diffusivities of water in PDMS are also in qualitative agreement with simulations that predict a marked increase (~15%) in water diffusivity near hydrophobic interfaces.[16] Interestingly, this result indicates that the PDMS polymer chains do not significantly limit the mean free path of water molecules and that tortuosity effects are minimal, likely because the PDMS chains are effectively in a liquid state.

Diffusivities in mixtures generally vary with composition, often in complicated ways that depend on the averaged interactions of the different molecular species. For example, Figure 2 shows a plot of the self-diffusivities of THF,

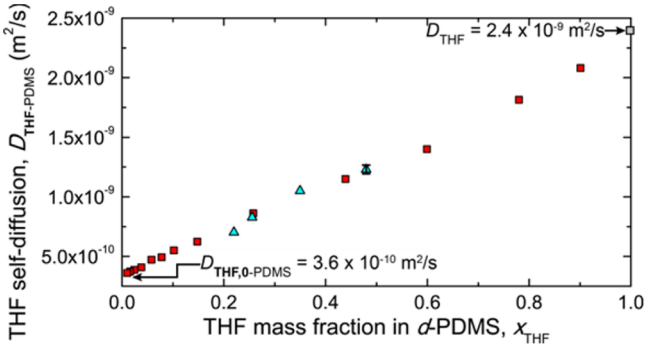

Figure 2. Self-diffusivities of THF in binary mixtures of perdeuterated d-PDMS, plotted as a function of THF mass fraction, as measured by ^{1}H PFG NMR at 20 °C: neat THF (gray square) and as a function of THF mass fraction in un-cross-linked d-PDMS (red squares) and cross-linked PDMS (blue triangles). The uncertainties are approximately the size of the data points.

$D_{THF-PDMS}$, in un-cross-linked d-PDMS (red squares), as measured by ^{1}H PFG NMR for a range of binary THF−PDMS compositions spanning 1−90 wt % THF; the same data are also plotted as a function of d-PDMS volume fraction in Figure S1 of the Supporting Information. Over this composition range, THF self-diffusion coefficients closely follow a linear relationship. The smaller THF diffusivities measured at low THF mass fractions in PDMS are consistent with PDMS polymer chains obstructing the diffusion paths of dilute solvent molecules.[17] The overlap concentration is estimated to be 0.85 mass fraction THF (see Supporting Information), above which the PDMS polymers can be considered noninteracting and dilute in the THF solvent. The results indicate that at lower THF concentrations (< 0.85) the PDMS chains are nonaggregated and dispersed. Separate measurements establish that these quantitative results are independent of PDMS cross-linking (blue triangles, see also Figure S2). The linear relationship for $D_{THF-PDMS}$ over the full composition range suggests that THF and PDMS form ideal binary solution mixtures,[18] indicating that THF diffusion in PDMS is governed principally by excluded volume and van der Waals interactions, consistent with the absence of significant H-bonding between THF and PDMS.

Although THF and water are miscible, their respective self-diffusion coefficients exhibit significantly more complicated composition dependences in their binary mixtures compared to the THF−PDMS system. As shown in Figure 3A for compositions ranging from pure water to pure THF, the bicomponent self-diffusivities (left vertical axis) of both water (yellow circles) and THF (red squares) vary nonlinearly with THF mole fraction. The binary self-diffusion coefficients for both water ($D_{water-THF}$) and THF ($D_{THF-water}$) are highest at very low water concentrations. Minimum values are also

DOI: 10.1021/acs.macromol.6b01514
Macromolecules 2016, 49, 6910−6917

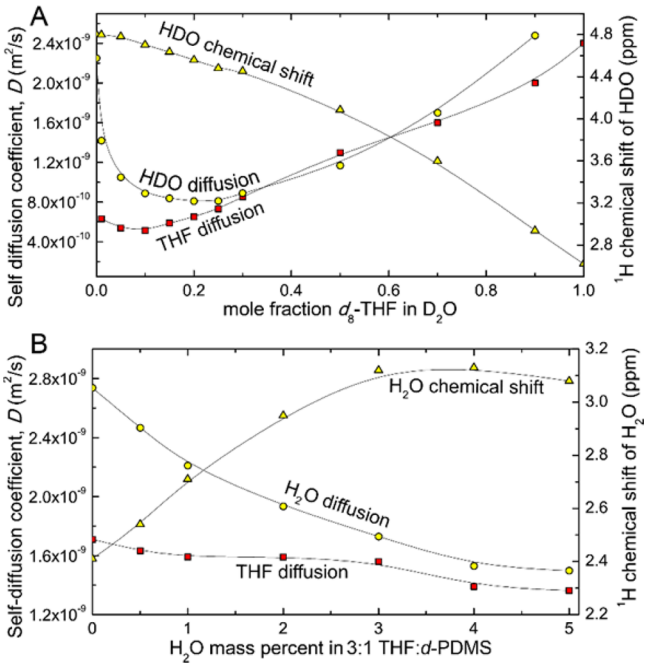

Figure 3. Self-diffusion coefficients of water (or HDO) and THF measured by ^{1}H PFG NMR at 20 °C, plotted together with ^{1}H isotropic chemical shifts for water in (A) binary solutions of 99.5% perdeuterated d_8-THF and D_2O and (B) ternary 25% perdeuterated-PDMS/75% d_8-THF mixtures, containing small amounts of H_2O: water self-diffusivities (yellow circles), THF self-diffusivities (red squares), and water ^{1}H chemical shifts (yellow triangles). The uncertainties are smaller than the size of the data points. Lines are shown to guide the eye.

measured for their respective self-diffusivities ($D_{water-THF}$ = 8.0 × 10^{-10} m^2/s and $D_{THF-water}$ = 5.0 × 10^{-10} m^2/s) at similar THF mole fractions of 0.20 and 0.10, respectively. The rapid decrease in the water self-diffusion coefficient at low THF concentration is consistent with stronger hydrogen bonding among water molecules that are thought to involve clathrate-like structures of H-bonded water around the relatively hydrophobic THF molecules.[19,20] Similar diffusion minima have been observed for other binary aqueous mixtures, which are linked to the formation of water−cosolvent solvation structures that limit molecular mobilities.[20,21] Recent simulations have suggested that similar segregated structures can form in binary water−methanol mixtures due to a loss of rotational entropy of the cosolvent molecules.[22]

Molecular-level insights into the solubility and diffusion properties of complicated water−polydimethylsiloxane binary and water−polydimethylsiloxane−THF ternary systems can be obtained by measuring and correlating the isotropic ^{1}H chemical shifts of water in the respective mixtures. The ^{1}H isotropic chemical shift is sensitive to average molecular environments, including hydrogen-bonding interactions, in the solutions.[20,23] For example, Figure 3A shows a plot of the ^{1}H chemical shift (right vertical axis, yellow triangles) measured for water, which progressively decreases as the THF mole fraction (X_{THF}) increases. For low THF contents (X_{THF} < 0.1), the ^{1}H chemical shift is close to that of pure water (4.6−4.8 ppm), indicating that the average hydrogen-bonding environment of water molecules is minimally perturbed, despite the large (60%) decrease in its self-diffusion coefficient.

These analyses indicate that the solvation environments of the THF molecules do not significantly perturb local water structure, though do reduce macroscopic water mobility. This conclusion is consistent with X-ray scattering analyses for the same compositions that indicate the solvation structure is similar to that of pure water.[19] For higher THF contents (0.3 < X_{THF} < 1), however, the ^{1}H chemical shift of water decreases dramatically from 4.4 to 2.7 ppm, reflecting reduced H-bonding interactions for water molecules in comparatively hydrophobic THF. Importantly, the decrease in the ^{1}H isotropic chemical shift of water in binary mixtures with THF is correlated with an increase in both the water and THF self-diffusion coefficients. This suggests that reduced hydrogen-bonding and formation of local solution structure(s) similar to that of concentrated THF enable water molecules to diffuse more rapidly.

For intermediate THF contents, 0.1 < X_{THF} < 0.3, the water ^{1}H chemical shift decreases slightly (4.6 to 4.4 ppm), while the diffusivities of both THF and water pass through minima with respect to THF mole fraction. This behavior is consistent with dynamic transitional structures within binary THF−water solutions over the range 10−20 mol % THF, including transient local configurations in which the hydrophobic THF moieties are directed away from H-bonding water molecules, a result that is also supported by X-ray[19] and theoretical analyses.[22] The transitional structure at these concentrations is also suggested by a maximum in the viscosity of water−THF mixtures.[24−26] Interestingly, the ^{1}H chemical shifts associated with the THF moieties remained constant within experimental error over the composition range examined; more precise measurements reported by Mizuno et al. indicate a slight decrease of the THF ^{1}H chemical shift (<0.2 ppm) as the THF concentration increases.[27] The complicated composition dependences of THF and water self-diffusion coefficients in their binary mixtures can thus be linked to differences in local hydrogen bonding, as manifested by the ^{1}H isotropic chemical shifts of water in the solutions.

Insights obtained for the binary PDMS−THF and water−THF mixtures can be applied to the ternary PDMS−water−THF system to better understand its more complicated bulk properties. Ternary mixtures were examined by adding small amounts of water to three binary mixtures, specifically 3:1, 1:1, and 1:3 THF:*d*-PDMS by mass mixtures. As expected, the saturation concentration of water decreased rapidly, as the amount of THF in the ternary mixture decreased. For 3:1 THF:*d*-PDMS, the saturation concentration was approximately 5 wt % water, which decreased to 0.9 and 0.5 wt % for the 1:1 and 1:3 THF:*d*-PDMS mixtures, respectively. The diffusivities and ^{1}H chemical shifts of the component species were monitored as functions of water content in each of these mixtures. Figure 3B shows plots of the self-diffusivities of water and THF for a mixture with a 3:1 mass ratio of THF to *d*-PDMS (left vertical axis). Similar to the diffusion behaviors of water and THF in their respective binary mixtures (Figure 3A), the self-diffusivities of water and THF both decrease, as the amount of water in the THF-*d*-PDMS−water ternary mixtures is increased. The diffusion coefficient of water decreases significantly from (2.7 ± 0.1) × 10^{-9} to (1.5 ± 0.1) × 10^{-9} m^2/s, as the amount of water increases from 0.01 to 5 wt %. The diffusion coefficient of THF decreases modestly, from (1.7 ± 0.1) × 10^{-9} to (1.4 ± 0.1) × 10^{-9} m^2/s over the same composition range. The decreases in the diffusivities of both THF and H_2O at higher H_2O contents indicate that the water

DOI: 10.1021/acs.macromol.6b01514
Macromolecules 2016, 49, 6910−6917

molecules interact primarily with THF in the ternary PDMS−H_2O−THF mixture.

Additional evidence that water interacts primarily with THF in the ternary mixtures is provided by solution-state ^{1}H NMR analyses. Specifically, comparisons of the isotropic ^{1}H chemical shift values of water in the binary water-THF versus the ternary PDMS−water−THF systems (Figure 3A,B) reflect the different extents of water H-bonding in the mixtures; stronger hydrogen bonding is generally associated with displacements of the ^{1}H NMR signals to higher frequencies.[20] For example, bulk H_2O yields a ^{1}H NMR signal at ∼4.8 ppm that is characteristic of its strong hydrogen bonds. By comparison, dilute water dissolved in THF or dispersed in PDMS results in ^{1}H signals at 2.63 or 1.76 ppm, respectively, consistent with reduced hydrogen bonding of water in its binary mixtures with these cosolvents.

Interestingly, at low water concentrations (∼0.01 wt % in the ternary system), the water ^{1}H chemical shift was measured to be 2.4 ppm (Figure 3B), which is between the values for the two dilute binary water−THF and water−PDMS mixtures and reflects an intermediate extent of water interaction with THF and PDMS. The ^{1}H chemical shift values thus indicate that water molecules experience average H-bonding environments in the ternary mixture that are similar to binary water−THF mixtures with the same water-to-THF ratio. In contrast, water and PDMS appear to interact less in ternary PDMS−water−THF mixtures, as reflected by water ^{1}H chemical shifts between 2.4 and 3.1 ppm that would otherwise be closer to the value measured in PDMS (1.76 ppm).

Conversely, at higher ternary water concentrations (>0.5 wt %), the isotropic ^{1}H chemical shift varies with the water-to-THF mass ratio in a manner similar to that of the binary system, increasing as the water content increases. Specifically, for 1 wt % water in the ternary mixture, the measured isotropic ^{1}H chemical shift of 2.70 is approximately the same as the weighted-average value of 2.77 ppm. This is similarly the case for 2 and 3 wt % water mixtures, for which the measured values of 2.94 and 3.11 ppm compare closely to the weighted-average values of 2.90 and 3.06 ppm, respectively. Thus, all of the observed ^{1}H chemical shift values for H_2O are within a fraction of a ppm to their weighted-average values, indicating that water molecules experience H-bonding environments in the ternary mixture that are similar to what they would experience in a binary water−THF mixture with the same water-to-THF mass ratio. Therefore, these chemical shift values indicate that the higher water solubility in the THF−PDMS mixtures is due to favorable interactions, specifically hydrogen-bonding, between water and THF.

Similar trends in the diffusion coefficients and chemical shifts as observed for the 3:1 THF-to-*d*-PDMS sample are observed for 1:1 and 1:3 THF-to-*d*-PDMS mixtures when the water contents are systematically increased. Figure 4A,B shows plots of the self-diffusion coefficients of water (yellow circles) and THF (red squares) for the 1:1 and 1:3 mixtures, respectively. Whereas the THF self-diffusion coefficients did not vary significantly over the range of compositions examined, the water self-diffusivities were significantly lower in both the 1:1 and 1:3 mixtures and varied similarly as for the 3:1 solution. The water self-diffusion coefficients in the three mixtures also exhibit similar values of approximately 1.5×10^{-9} m^2/s at their respective saturation compositions. The isotropic ^{1}H chemical shift values of water in the 1:1 and 1:3 THF-to-*d*-PDMS mixtures also follow similar trends to that observed in the 3:1 mixture, reflecting similar associated molecular interactions

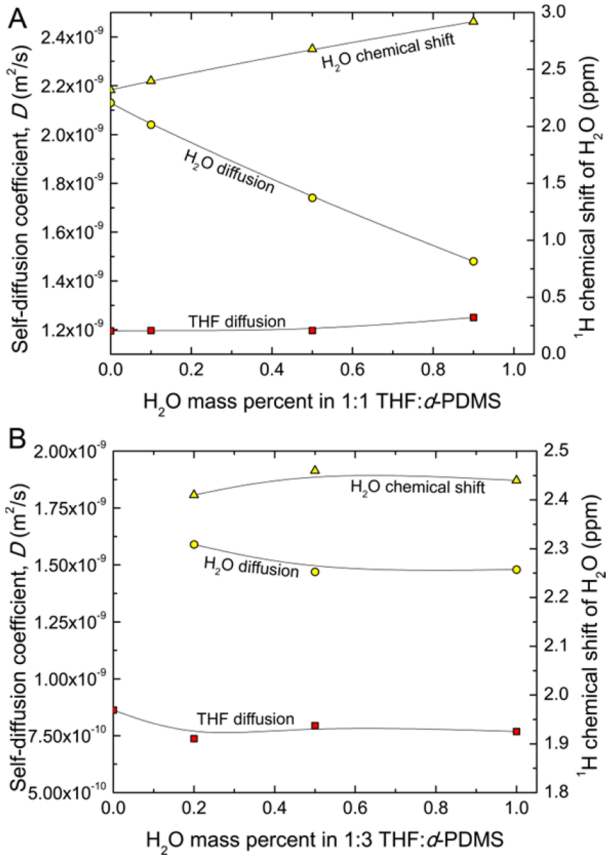

Figure 4. Plots of the self-diffusion coefficients of water and THF and the isotropic ^{1}H chemical shift of water in mixtures of (A) 1:1 THF:*d*-PDMS and (B) 1:3 THF:*d*-PDMS in the presence of small amounts of water at 20 °C. Both panels use the same symbol and color scheme: red squares correspond to THF diffusivities, yellow circles to water diffusivities, and yellow triangles to the isotropic ^{1}H chemical shifts of water. For the 1:1 THF:*d*-PDMS mixture, the saturation concentration of water is about 0.9 wt %, while for the 1:3 THF:*d*-PDMS mixture, it is about 0.5 wt % water; above these concentrations, water begins to phase-separate. The uncertainties are smaller than the size of the data points. Lines are shown to guide the eye.

across the ternary composition range. For the 1 THF:1 PDMS mixture (Figure 4A), at low water contents, the ^{1}H chemical shift was measured to be lower than for dilute water−THF mixtures, indicating unfavorable water interactions with *d*-PDMS as well as the THF molecules. At higher water contents, the observed water ^{1}H chemical shift was similar to the expected values, based on its molar ratio with THF (2.67 ppm versus 2.73 ppm, respectively, for 0.5 wt % and 2.91 ppm versus 2.81 ppm, respectively, for 0.9 wt %). This suggests that for higher water contents water molecules are mostly proximate to THF molecules, rather than *d*-PDMS, as was found for the 3 THF:1 PDMS mixture. The isotropic ^{1}H chemical shift data indicate that, in both the 1:1 and 3:1 mixtures, sufficient THF is present for water molecules to interact almost exclusively with THF molecules at higher water contents. By comparison, for the 1 THF:3 PDMS mixture (Figure 4B), only small differences were observed in the water ^{1}H chemical shifts over the narrow composition range in which the solutions were miscible. The values of the water ^{1}H chemical shift for this 1 THF:3 PDMS mixture were slightly smaller than for dilute water in THF, consistent with water molecules interacting mostly with THF molecules and modestly with the hydrophobic *d*-PDMS.

DOI: 10.1021/acs.macromol.6b01514
Macromolecules 2016, 49, 6910−6917

Collectively, these results indicate that the water is solubilized primarily by THF, rather than PDMS, especially at water contents that significantly exceed the solubility limit of water in PDMS. The complex interactions among water, THF, and PDMS molecules account for their relative solubilities and complicated self-diffusion behaviors in their ternary mixtures.

Further insights on how molecular interactions influence the macroscopic properties of ternary PDMS−water-THF mixtures are gained by quantifying the interaction forces at PDMS surfaces in the presence of the two cosolvents. By using the surface forces apparatus (SFA), direct force measurements can be correlated with the respective self-diffusivities and ^{1}H chemical shifts of the cosolvent species. Using a recently derived general interaction potential,[9,10,28,29] the hydrophobic interaction energy, W_H, decays exponentially with the film separation d and depends on the PDMS−water interfacial tension γ_i, the nondimensional Hydra parameter Hy, and decay length D_H (generally $D_H \sim 1$ nm for extended surfaces):

$$W_H = -2\gamma_i Hy e^{-d/D_H} \quad (1)$$

The Hydra parameter Hy is related to the interfacial hydrophobicity and can be thought of as the area fraction of hydrophobic groups at an interface.[9,10,29] For two PDMS surfaces interacting across an aqueous solution, γ_i = 44 mJ/m^2,[30] a strongly attractive hydrophobic interaction is expected, $Hy \approx 1$,[10] corresponding to essentially complete phase separation. The measurements of the interaction forces between two PDMS interfaces separated by pure water indicate that the main contribution to the overall interaction is the hydrophobic interaction (see Figure S3), with small contributions from van der Waals forces as well.[10] The van der Waals adhesion was calculated as shown in the Supporting Information and is relatively weak compared to the measured adhesion in pure water. Therefore, the magnitude of the adhesion energy approaches $W_0 = 2\gamma_i Hy$ at molecular contact for two hydrophobic interfaces. For two PDMS interfaces in water, the theoretical adhesion energy is thus W_0 = 88 mJ/m^2. According to the Johnson−Kendall−Roberts theory,[31] the adhesion energy can be calculated from the measured adhesion force $W_{ad} = 2F_{ad}/3\pi R$. The value of Hy can then be evaluated for different solvent compositions by measuring the adhesion energy for different compositions in water−THF mixtures.

The adhesion energy between PDMS films decreases as the aqueous solution becomes more concentrated in THF, reflecting the complicated influences of both the hydrophobic and hydrogen-bonding characters of THF. As shown in Figure 5, the magnitude of the adhesion energy, W_{ad}, along with the corresponding value of Hy, both decrease accordingly, as the THF concentration increases. The average measured adhesion energy is W_{ad} = 94 ± 20 mJ/m^2 for 0% THF, in good agreement with the expected thermodynamic value of W_0 = 88 mJ/m^2. For PDMS thin films in water, Hy is determined to be 1.07 ± 0.23, consistent with their highly hydrophobic characters. By comparison, for PDMS films separated by an aqueous solution with 10 mol % THF, the adhesion energy was measured to be dramatically lower, corresponding to values of W_{ad} = 31 ± 10 mN/m and Hy = 0.34 ± 0.13, both of which reflect significantly reduced hydrophobic contributions to the overall interaction energy. For 20 mol % THF, the values of W_{ad} = 7 ± 2 mJ/m^2 and Hy = 0.05 ± 0.03 reflect nearly negligible contributions from hydrophobicity, as similarly observed at higher THF concentrations: Hy = 0.03 ± 0.01 for 30 mol % THF and Hy = 0.04 ± 0.04 for 50 mol % THF. Thus, above 20 mol % THF, Hy approaches zero, as the adhesion approaches the expected van der Waals adhesion (Figure 5).

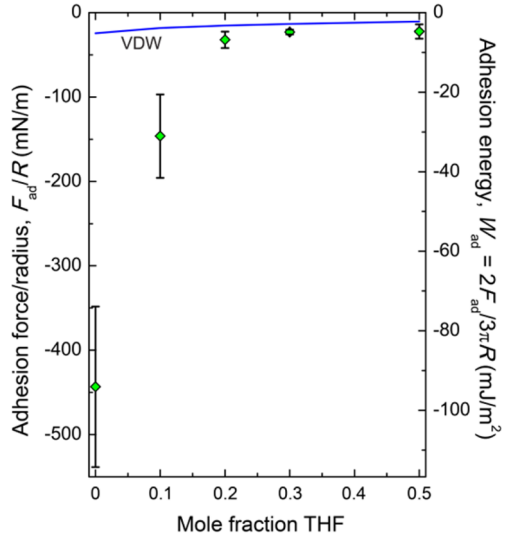

Figure 5. Average adhesion forces (left vertical axis) and energies (right vertical axis) measured by SFA as functions of THF mole fraction at 21 °C. The blue line labeled "VDW" indicates the theoretical composition-dependent van der Waals adhesion.

Interestingly, Hy decreases to effectively zero at ∼20 mol % THF, the same concentration at which minimums are observed for the self-diffusivities of THF and H_2O in the water−THF binary mixtures. The minimum values of the self-diffusivities, as discussed above, manifest stronger H-bonded-liquid structures in the binary THF−water system compared to water−PDMS. Therefore, it appears that bulk-phase hydrogen bonding directly influences the hydrophobic interactions by allowing similar H-bonding to occur near the PDMS interface, reducing otherwise strong hydrophobic adhesion between PDMS surfaces. While the exact composition likely varies within the PDMS films, the PDMS surfaces are in contact with bulk-like liquid films, even approaching molecular dimensions.[32]

The force−distance curves measured between two PDMS interfaces for different THF−water compositions provide quantitative insights into PDMS swelling and chain−solvent interactions, as shown in Figure 6. The adhesion force F_{ad}/R is determined from these curves as the minimum value before the final jump-out from contact. Adhesive contact of the two PDMS films in pure water corresponds to the case where $d = 0$; the combined thickness of the two PDMS layers in contact is $2T \approx 12$ nm. Addition of THF to the aqueous solution causes the thicknesses of the PDMS films to become larger, while the adhesion energy W_{ad} decreases. Thicker films are observed when contact of the films occurs at distances $d > 0$ for increasing THF concentration. The SFA results indicate that THF and water penetrate into the PDMS films, consistent with the ^{1}H NMR chemical shift measurements in Figure 3B. However, no evidence for entropic repulsion is observed.[9,10] It is noteworthy that, for aqueous solutions with 10−30 mol % THF, a 5−10 nm extension of the force−distance curve is observed in Figure 6 before jump-out from contact, as the PDMS films were separated from each other, which is characteristic of a bridging-type force−distance profile. This indicates that PDMS chains extend from the surfaces and into

DOI: 10.1021/acs.macromol.6b01514
Macromolecules 2016, 49, 6910−6917

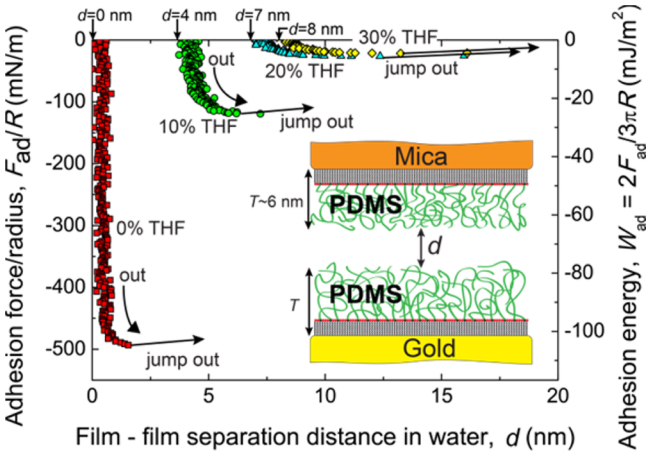

Figure 6. Representative SFA force−distance curves and associated adhesion energies for retracting PDMS surfaces separated by water−THF mixtures containing 0%, 10%, 20%, or 30% THF at 21 °C.

the solvent environment before the final jump-out,[33] consistent with a reduction of the energy needed to solubilize PDMS chain segments at higher THF concentrations. The SFA measurements of PDMS films in binary water−THF solutions thus establish that THF and water can penetrate into the PDMS films as depicted in Figure 1B, resulting in dramatically reduced adhesion between the films.

The combined observations from ^{1}H diffusion NMR, ^{1}H isotropic chemical shift, and SFA analyses provide insights about the influence of solvent structure on hydrophobic interactions. These results indicate that the addition of THF alters the hydrogen-bonding structure of water, both in bulk solution and at a PDMS interface, as shown schematically in Figure 1. Water molecules in general cannot establish a hydrogen-bonding network with extended PDMS interfaces, as manifested by a strongly attractive hydrophobic interaction measured by SFA. These results are supported by molecular simulations, which show increased interfacial fluctuations, water dynamics, and proximity to a liquid−vapor phase transition near hydrophobic interfaces.[4,16,34] In contrast, THF forms hydrogen bonds with water molecules, modifying the interfacial solvation structure, so that the overall hydrophobic interaction decreases. Our results therefore suggest that local fluctuations of water molecules, due to hydrophobicity, would be significantly damped in the presence of THF. The multicomponent ^{1}H diffusion NMR and isotropic chemical shift measurements reveal why this is the case: in ternary PDMS−THF−water mixtures, the influences of the highly unfavorable water−PDMS interactions are substantially mitigated by the presence of THF, which interacts favorably with the hydrophobic PDMS and can hydrogen bond with water. Under such circumstances, hydrophobic interactions between the PDMS interfaces are dramatically reduced and hydrophobic influences essentially disappear at ca. 20 mol % THF. This is consistent with the influence of hydrogen bonding among water and THF molecules on their long-range mobilities (as measured by ^{1}H PFG diffusion NMR) and on the interfacial hydrophobicity (as probed by the SFA adhesion measurements). Quantifying interfacial hydrophobicity with *Hy* aids the analyses, forming the basis by which composition-dependent hydrogen-bonding and interaction forces between hydrophobic surfaces are correlated, here, for the THF−water−PDMS system.

In summary, the self-diffusivities and ^{1}H chemical shifts of water and THF in binary and ternary solutions with silicone polymers have been correlated with the hydrophobic adhesion energies between hydrophobic polydimethylsiloxane thin films. These results elucidate the molecular factors that account for the suppression of phase separation in complicated ternary polydimethylsiloxane−water−THF mixtures compared to binary polydimethylsiloxane−water systems. ^{1}H PFG diffusion and chemical shift NMR measurements of ternary PDMS, water, and THF mixtures establish that water molecules are solubilized by THF and interact weakly with PDMS. In the presence of THF, water diffusion in PDMS is significantly lower than that for water in pure PDMS, which correlates with significant hydrogen bonding between water and THF molecules. It is noteworthy that recent experimental work has reported the disappearance of hydrophobic adhesion in methanol−water solutions[35] at a similar composition where segregated structures were separately found in bulk solution by simulations[22] and where diffusion minima were observed by ^{1}H PFG NMR.[20] This provides corroborating evidence that these properties are general and interrelated effects of cosolvents on hydrophobicity.

When bulk liquid structures of water−cosolvent mixtures are dominated by water, hydrophobic interactions can still persist. At higher cosolvent concentrations, a threshold is eventually reached where water preferentially hydrogen bonds with THF, and hydrophobic interactions between PDMS films are diminished congruently. Therefore, we have shown that local hydrogen bonding can have a dramatic influence on the solubilities, diffusivities, and thin-film interaction forces in ternary polydimethylsiloxane−water−cosolvent mixtures, as governed by the relative hydrophobicities of the respective components, as depicted schematically in Figure 1B. These effects are expected to be important to the formation of supramolecular assemblies of nanoscale materials and in the engineering of oriented polymer mesostructures, where the behaviors, properties, and interactions of polymer−water−cosolvent mixtures are of broad interest.

■ ASSOCIATED CONTENT

Supporting Information

The Supporting Information is available free of charge on the ACS Publications website at DOI: 10.1021/acs.macromol.6b01514.

Diffusion analyses of cross-linked polydimethylsiloxane−THF solutions; diffusion of *d*-PDMS−THF solutions as a function of polymer volume fraction; diffusion analyses of water in ternary 1:1 and 1:3 THF:*d*-PDMS mixtures; interactions between symmetric PDMS thin films (PDF)

■ AUTHOR INFORMATION

Corresponding Author

*E-mail bradc@engineering.ucsb.edu (B.F.C.).

Notes

The authors declare no competing financial interest.

■ ACKNOWLEDGMENTS

The authors thank D. Topgaard for helpful discussions. This work was supported in part by the U.S. National Science Foundation under Grant CHE-1059108 and by the Institute for Collaborative Biotechnologies through Grant W911NF-09-0001 from the U.S. Army Research Office. The content of

DOI: 10.1021/acs.macromol.6b01514
Macromolecules 2016, 49, 6910−6917

the information does not necessarily reflect the position or the policy of the U.S. Government, and no official endorsement should be inferred. The perdeuterated polydimethylsiloxane sample was synthesized at the Center for Nanophase Materials at Oak Ridge National Laboratory supported by the U.S. Department of Energy. The NMR measurements were conducted using the Central Facilities of the UCSB Materials Research Laboratory supported by the MRSEC program of the U.S. NSF (Award DMR-1121053). S.H.D. was supported by LabEX ENS-ICFP: ANR-10-LABX-0010/ANR-10-IDEX-0001-02 PSL.

REFERENCES

(1) Valle, K.; Belleville, P.; Pereira, F.; Sanchez, C. Hierarchically structured transparent hybrid membranes by in situ growth of mesostructured organosilica in host polymer. *Nat. Mater.* **2006**, *5* (2), 107−111.
(2) Einstein, A. Motion of suspended particles on the kinetic theory. *Ann. Phys.* **1905**, *322* (8), 549−560.
(3) Luzar, A.; Chandler, D. Hydrogen-bond kinetics in liquid water. *Nature* **1996**, *379* (6560), 55−57.
(4) Chandler, D. Interfaces and the driving force of hydrophobic assembly. *Nature* **2005**, *437* (7059), 640−647.
(5) Beltzung, M.; Picot, C.; Rempp, P.; Herz, J. Investigation of the conformation of elastic chains in poly(dimethylsiloxane) networks by small-angle neutron scattering. *Macromolecules* **1982**, *15* (6), 1594−1600.
(6) Bellas, V.; Iatrou, H.; Hadjichristidis, N. Controlled anionic polymerization of hexamethylcyclotrisiloxane. Model linear and miktoarm star Co- and terpolymers of dimethylsiloxane with styrene and isoprene. *Macromolecules* **2000**, *33* (19), 6993−6997.
(7) Pelta, M. D.; Morris, G. A.; Stchedroff, M. J.; Hammond, S. J. A one-shot sequence for high-resolution diffusion-ordered spectroscopy. *Magn. Reson. Chem.* **2002**, *40*, S147−S152.
(8) Stejskal, E. O.; Tanner, J. E. Spin diffusion measurements: spin echoes in the presence of a time-dependent field gradient. *J. Chem. Phys.* **1965**, *42* (1), 288−292.
(9) Donaldson, S. H., Jr.; Das, S.; Gebbie, M. A.; Rapp, M.; Jones, L. C.; Roiter, Y.; Koenig, P. H.; Gizaw, Y.; Israelachvili, J. N. Asymmetric electrostatic and hydrophobic-hydrophilic interaction forces between mica surfaces and silicone polymer thin films. *ACS Nano* **2013**, *7* (11), 10094−10104.
(10) Donaldson, S. H., Jr.; Royne, A.; Kristiansen, K.; Rapp, M. V.; Das, S.; Gebbie, M. A.; Lee, D. W.; Stock, P.; Valtiner, M.; Israelachvili, J. Developing a general interaction potential for hydrophobic and hydrophilic interactions. *Langmuir* **2015**, *31* (7), 2051−2064.
(11) Israelachvili, J.; Min, Y.; Akbulut, M.; Alig, A.; Carver, G.; Greene, W.; Kristiansen, K.; Meyer, E.; Pesika, N.; Rosenberg, K.; Zeng, H. Recent advances in the surface forces apparatus (SFA) technique. *Rep. Prog. Phys.* **2010**, *73* (3), 036601.
(12) Israelachvili, J. Thin-film studies using multiple-beam interferometry. *J. Colloid Interface Sci.* **1973**, *44* (2), 259−272.
(13) Watson, J. M.; Baron, M. G. The behaviour of water in poly(dimethylsiloxane). *J. Membr. Sci.* **1996**, *110* (1), 47−57.
(14) Randall, G. C.; Doyle, P. S. Permeation-driven flow in poly(dimethylsiloxane) microfluidic devices. *Proc. Natl. Acad. Sci. U. S. A.* **2005**, *102* (31), 10813−10818.
(15) Holz, M.; Heil, S. R.; Sacco, A. Temperature-dependent self-diffusion coefficients of water and six selected molecular liquids for calibration in accurate H-1 NMR PFG measurements. *Phys. Chem. Chem. Phys.* **2000**, *2* (20), 4740−4742.
(16) Jamadagni, S. N.; Godawat, R.; Garde, S. How surface wettability affects the binding, folding, and dynamics of hydrophobic polymers at interfaces. *Langmuir* **2009**, *25* (22), 13092−13099.
(17) Pickup, S.; Blum, F. D. Self-diffusion of toluene in polystyrene solutions. *Macromolecules* **1989**, *22* (10), 3961−3968.
(18) Weingärtner, H. The molecular description of mutual diffusion processes in liquid mixtures. In *Diffusion in Condensed Matter*, 1st ed.; Heitjans, P., Kärger, J., Eds.; Springer: Houten, The Netherlands, 2005; pp 555−578.
(19) Takamuku, T.; Nakamizo, A.; Tabata, M.; Yoshida, K.; Yamaguchi, T.; Otomo, T. Large-angle X-ray scattering, small-angle neutron scattering, and NMR relaxation studies on mixing states of 1,4-dioxane-water, 1,3-dioxane-water, and tetrahydrofuran-water mixtures. *J. Mol. Liq.* **2003**, *103*, 143−159.
(20) Price, W. S.; Ide, H.; Arata, Y. Solution dynamics in aqueous monohydric alcohol systems. *J. Phys. Chem. A* **2003**, *107* (24), 4784−4789.
(21) Leaist, D. G.; MacEwan, K.; Stefan, A.; Zamari, M. Binary mutual diffusion coefficients of aqueous cyclic ethers at 25° C. Tetrahydrofuran, 1,3-dioxolane, 1,4-dioxane, 1,3-dioxane, tetrahydropyran, and trioxane. *J. Chem. Eng. Data* **2000**, *45* (5), 815−818.
(22) Pascal, T. A.; Goddard, W. A. Hydrophobic segregation, phase transitions and the anomalous thermodynamics of water/methanol mixtures. *J. Phys. Chem. B* **2012**, *116*, 13905−13912.
(23) Nose, A.; Hojo, M.; Ueda, T. Effects of salts, acids, and phenols on the hydrogen-bonding structure of water-ethanol mixtures. *J. Phys. Chem. B* **2004**, *108* (2), 798−804.
(24) Saleh, M. A.; Akhtar, S.; Ahmed, M. S.; Uddin, M. H. Viscosities of aqueous solutions of dimethylsulfoxide, 1,4-dioxane and tetrarydrofuran. *Phys. Chem. Liq.* **2001**, *39* (5), 551−563.
(25) Nayak, J. N.; Aralaguppi, M. I.; Naidu, B. V. K.; Aminabhavi, T. M. Thermodynamic properties of water plus tetrahydrofuran and water plus 1,4-dioxane mixtures at (303.15, 313.15, and 323.15) K. *J. Chem. Eng. Data* **2004**, *49* (3), 468−474.
(26) Hayduk, W.; Laudie, H.; Smith, O. H. Viscosity, freezing-point, vapor-liquid equilibria, and other properties of aqueous tetrahydrofuran solutions. *J. Chem. Eng. Data* **1973**, *18* (4), 373−376.
(27) Mizuno, K.; Masuda, Y.; Yamamura, T.; Kitamura, J.; Ogata, H.; Bako, I.; Tamai, Y.; Yagasaki, T. Roles of the ether oxygen in hydration of tetrahydrofuran studied by IR, NMR, and DFT calculation methods. *J. Phys. Chem. B* **2009**, *113* (4), 906−915.
(28) Sanchez-Iglesias, A.; Grzelczak, M.; Altantzis, T.; Goris, B.; Perez-Juste, J.; Bals, S.; Van Tendeloo, G.; Donaldson, S. H.; Chmelka, B. F.; Israelachvili, J. N.; Liz-Marzan, L. M. Hydrophobic interactions modulate self-assembly of nanoparticles. *ACS Nano* **2012**, *6* (12), 11059−11065.
(29) Donaldson, S. H.; Lee, C. T.; Chmelka, B. F.; Israelachvili, J. N. General hydrophobic interaction potential for surfactant/lipid bilayers from direct force measurements between light-modulated bilayers. *Proc. Natl. Acad. Sci. U. S. A.* **2011**, *108* (38), 15699−15704.
(30) Chaudhury, M. K.; Whitesides, G. M. Direct measurement of interfacial interactions between semispherical lenses and flat sheets of poly(dimethylsiloxane) and their chemical derivatives. *Langmuir* **1991**, *7* (5), 1013−1025.
(31) Israelachvili, J. N. *Intermolecular and Surface Forces*; Academic Press: San Diego, CA, 2011.
(32) Horn, R. G.; Smith, D. T.; Haller, W. Surface forces and viscosity of water measured between silica sheets. *Chem. Phys. Lett.* **1989**, *162* (4−5), 404−408.
(33) Wong, J. Y.; Kuhl, T. L.; Israelachvili, J. N.; Mullah, N.; Zalipsky, S. Direct measurement of a tethered ligand-receptor interaction potential. *Science* **1997**, *275* (5301), 820−822.
(34) Jamadagni, S. N.; Godawat, R.; Garde, S.; Prausnitz, J. M. Hydrophobicity of proteins and interfaces: Insights from density fluctuations. *Annu. Rev. Chem. Biomol. Eng.* **2011**, *2*, 147−171.
(35) Ma, C. D.; Wang, C.; Acevedo-Velez, C.; Gellman, S. H.; Abbott, N. L. Modulation of hydrophobic interactions by proximally immobilized ions. *Nature* **2015**, *517* (7534), 347−350.

DOI: 10.1021/acs.macromol.6b01514
Macromolecules 2016, 49, 6910−6917

Supporting Information

Correlated diffusivities, solubilities, and hydrophobic interactions in ternary polydimethylsiloxane -water-tetrahydrofuran mixtures

Stephen H. Donaldson Jr.,[1,3] Justin P. Jahnke,[1] Robert J. Messinger,[1] Åsa Östlund,[1] David Uhrig,[2] Jacob N. Israelachvili,[1] Bradley F. Chmelka[1,*]

[1] Department of Chemical Engineering, University of California, Santa Barbara, California 93106-5080 U.S.A.

[2] Center for Nanophase Materials, Sciences Division, Oak Ridge National Laboratory P.O. Box 2008, Oak Ridge, Tennessee 37831 U.S.A.

[3] Departement de Physique, Ecole Normale Supérieure / PSL Research University, CNRS, 24 rue Lhomond, 75005 Paris, France

Self-diffusivities of THF in binary *d*-PDMS–THF mixtures as a function of polymer volume fraction

Due to the high viscosity of the *d*-PDMS, all samples were prepared on a mass basis for improved accuracy. To facilitate comparisons with data based on polymer volume fractions, self-diffusivities of THF in perdeuterated *d*-PDMS are plotted in Figure S1, as a function of *d*-PDMS volume fraction.

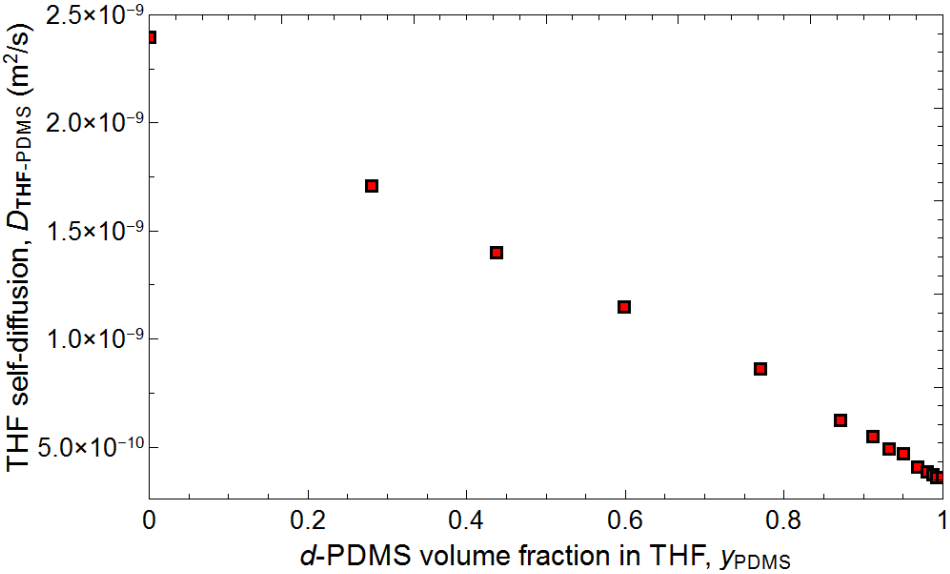

Figure S1. Self-diffusivities of THF in binary mixtures of perdeuterated *d*-PDMS, plotted as a function of *d*-PDMS volume fraction, as measured by ^{1}H PFG NMR at 20 °C. The same data are shown in Figure 2 of the main manuscript and in Figure S2 below, as a function of THF mass fraction in *d*-PDMS.

As THF is a good solvent for PDMS, no evidence of aggregation was anticipated or observed at higher THF contents. This is consistent with an estimate for the overlap concentration $c^*=3M_w/(4\pi N_A R_g^3)$,[3] where M_w is the polymer molecular weight, N_A is Avogadro's number, the radius of gyration is given by $R_g=ln^{1/2}/6^{1/2}$, and the literature value for segment length l = 5.6 Å. Using these values, the radius of gyration is estimated to be R_g = 4.2 nm for PDMS, leading to an estimated overlap concentration of c^*=134 g/L, which corresponds to a PDMS mass fraction of 0.15, below which the PDMS chains can be considered non-interacting and dilute.

Diffusion analyses of cross-linked polydimethylsiloxane-THF solutions

For many PDMS applications, including membrane separations and microfluidics,[1] cross-linked polymer gels are used rather than non-cross-linked liquids, so diffusion of THF within cross-linked PDMS was also examined. THF self-diffusion coefficients (Figure S2) were measured, as a function of composition for binary mixtures of 20-50 wt% THF in cross-linked (non-deuterated) PDMS (blue triangles) and non-cross-linked deuterated *d*-PDMS. All of the measured THF self-diffusion coefficients exhibited an approximately linear quantitative dependence on THF mass fraction that was essentially identical for the cross-linked and non-cross-linked PDMS. Only the concentration range between 20 wt% and 50 wt% THF could be measured for the non-deuterated cross-linked PDMS samples, because radiation damping during the NMR measurement prevented resolution of THF ^{1}H NMR signals outside this composition range. Based on the technical specifications provided for the Sylgard™ 184,[2] we estimate that there are approximately two functional branch points per polymer molecule. Assuming that all of the functional endgroups have reacted, we estimate a rough upper-bound for the cross-linking density to be about 1 cross-link for every 200 monomer sites. The actual value is probably significantly smaller than this value, and this is consistent with the observed liquid-like ^{1}H NMR spectra of the cross-linked samples. This low extent of cross-linking is consistent with the observed diffusivities not being significantly affected by the cross-linking. Much higher extents of cross-linking would likely have a larger effect on self-diffusion properties.

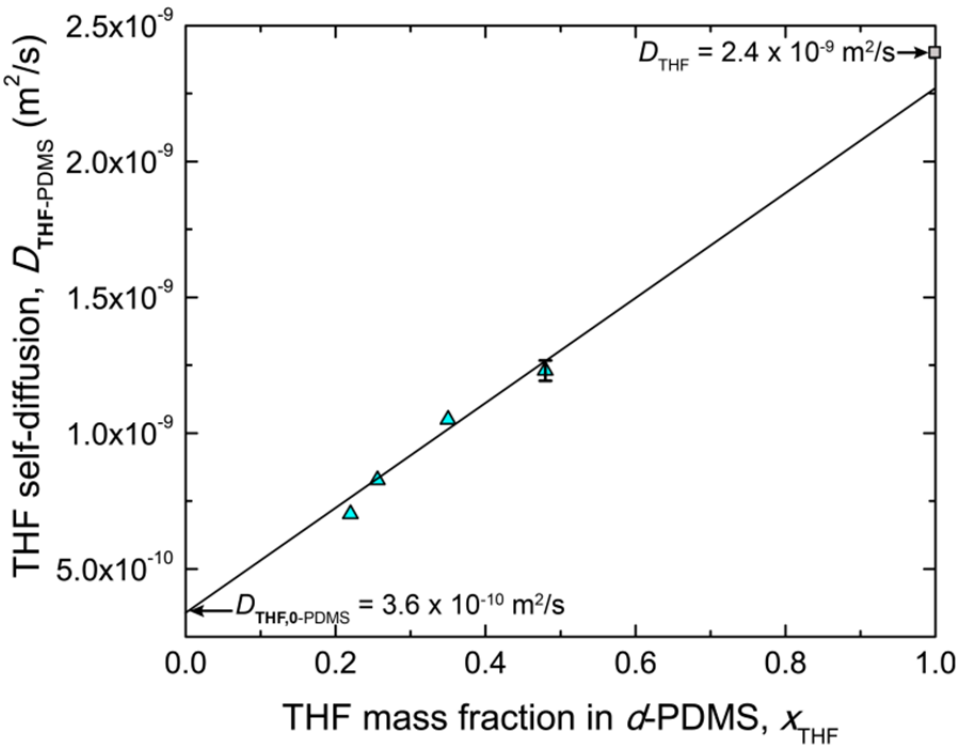

Figure S2. Self-diffusivities of THF in binary mixtures with cross-linked PDMS, plotted as a function of *d*-PDMS volume fraction, as measured by ^{1}H PFG NMR under ambient conditions. The line shows the approximate trend for non-cross-linked PDMS, the data for which is shown in Figure 2 of the main text. The cross-linked data lie on approximately the same trend line, indicating that PDMS cross-linking does not have a strong effect on molecular self-diffusion of THF under these conditions. The uncertainties are approximately the size of the data points, except for 0.50 THF, where the error bar is slightly larger, as shown.

Interactions between symmetric PDMS thin films

In SFA measurements of force-distance curves, values for the force F are typically scaled with respect to the radius of the curved interacting surface R, which allows results obtained from other techniques to be compared. The scaled force F/R can be used to calculate the interaction energy by using the Derjaguin approximation, $W = F/2\pi R$, and was measured during both approaches and separations of the surfaces, as a function of the film-film separation distance d. Typical force-distance curves exhibit repulsive forces as $F/R > 0$ and attractive forces as $F/R < 0$, as functions of the separation distance d between the surface films. As shown in Figure S3, the interactions between two PDMS films are fully attractive on both approach and separation. During approach, the surfaces jump-in from a large distance D_J = 22 nm to a hardwall distance D_H =13 nm, which corresponds to the combined thickness of the two PDMS films. The attractive force is clearly longer-ranged than the van der Waals forces for this system, as shown by the red

curve. During separation of the two surfaces, a very large adhesion energy of W_0 = 85 mJ/m^2 was measured, a value very close to the expected thermodynamic adhesion for two PDMS surfaces, i.e., $W_0 = 2\gamma$ = 88 mJ/m^2. This force run is representative for the PDMS-PDMS system in water.

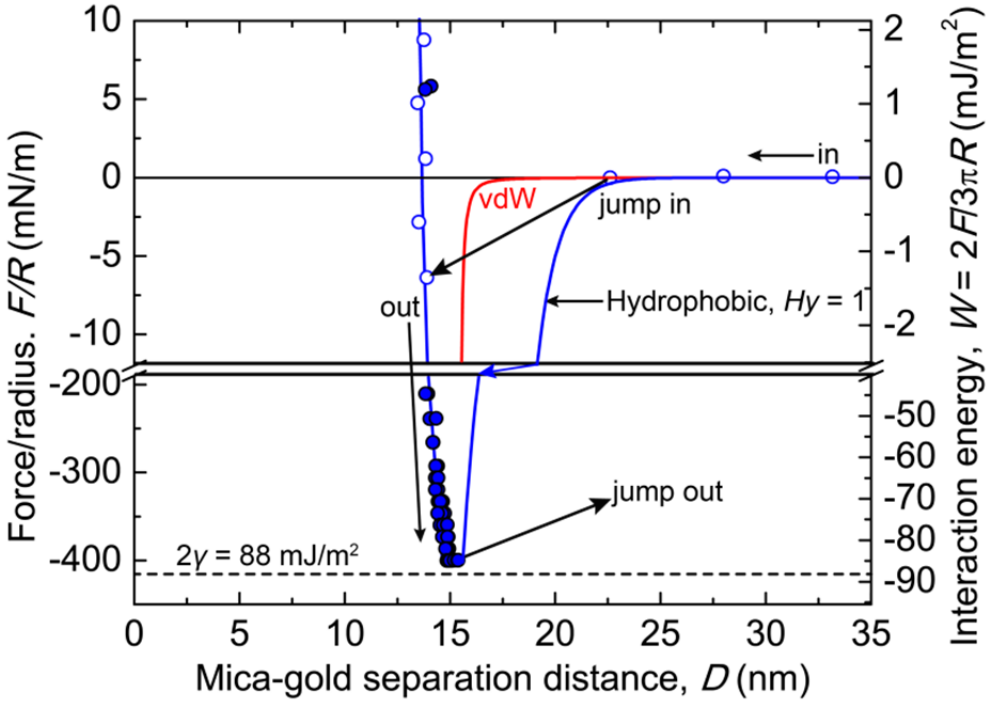

Figure S3. Interaction forces between two PDMS thin films in 1 mM NaCl aqueous solution at pH 3 and room temperature, as measured using the surface forces apparatus. The blue curve represents the maximum hydrophobic interaction using Equation 1 in the text, with Hy = 1, γ = 44 mJ/m^2, and D_H = 1 nm. The van der Waals forces according to Equations S2 and S3 below are shown for comparison as the red curve.

The interactions between PDMS films in aqueous solutions and aqueous-organic liquids mixtures can be described quantitatively by the total interaction energy W_{tot}, which consists of contributions from both hydrophobic and van der Waals interactions, $W_{tot} = W_H + W_{vdW}$, with the van der Waals interaction energy W_{vdW} calculated, as described below. The fit to the force data (Figure S3) establishes that the overall interaction potential is quantitatively well-described with Hy = 1, capturing both the long range attraction (d > 10 nm) and adhesion when the two films are in molecular contact (d = 0).

As shown above and in the main text of the manuscript, the interactions between the PDMS films are attractive during both approach and separation, with the main contribution arising from hydrophobic interactions. However, van der Waals interactions are always present between surfaces, and in this case the main contribution from van der Waals forces arises between the two

PDMS films. The PDMS films are sufficiently thick that the van der Waals force between the underlying mica and gold can be effectively ignored. The van der Waals interaction energy per unit area, W_{vdW}, between two PDMS films depends on the Hamaker constant of PDMS interacting with PDMS across water, A_{131}, and the separation distance D between the films, as shown in Equation S2:[3]

$$W_{vdW} = -\frac{A_{131}}{12\pi D^2} \tag{S2}$$

The Hamaker constant was calculated by using the following equation, as described in detail in reference.[4] Equation S3 comes from Lifshitz theory and is used to calculate the Hamaker constant for the symmetric case of two identical phases 1 interacting across medium 3:

$$A_{131} = \frac{3}{4}kT\left(\frac{\varepsilon_1 - \varepsilon_3}{\varepsilon_1 - \varepsilon_3}\right)^2 + \frac{3h\nu_e}{16\sqrt{2}}\frac{(n_1^2 - n_3^2)^2}{(n_1^2 + n_3^2)^{3/2}} \tag{S3}$$

In this case, the subscript 1 corresponds to PDMS, while subscript 3 corresponds to water. Using well-known values for the refractive indices and dielectric constants for PDMS and water, the Hamaker constant for PDMS films interacting across pure water, $A_{131} = 4\text{x}10^{-21}$ J. Tabulated data for the concentration dependent refractive indices[5] and dielectric constants[6] in water-THF mixtures were used to calculate the Hamaker constant for each composition. The van der Waals adhesion was estimated using Equation S2 and the Hamaker constant for each composition, at a cut-off distance of D = 0.165 nm. The line labelled "VDW" in Figure 4 (main manuscript text) corresponds to the van der Waals adhesion calculated in this way.

References

1. Lee, J. N.; Park, C.; Whitesides, G. M., Solvent compatibility of poly(dimethylsiloxane)-based microfluidic devices. *Anal. Chem.* **2003**, *75*(23), 6544-6554.
2. Flowers, G.; Switzer, S. T. *Background material properties of selected silicone potting compounds and raw materials for their substitutes*; Mason and Hanger-Silas Mason Co., Inc.: Amarillo, Texas (USA), 1978.
3. Ying Q.; Chu, B., Overlap concentration of macromolecules in solution, *Macromolecules* **1987**, *20*(2), 362-366
4. Israelachvili, J. N., *Intermolecular and Surface Forces,* 3rd Edition. Academic Press: San Diego, California, 2011.

5. Aminabhavi, T. M.; Gopalakrishna, B., Density, viscosity, refractive-index, and speed of sound in aqueous mixtures of *n,n*-dimethylformamide, dimethyl-sulfoxide, *n,n*-dimethylacetamide, acetonitrile, ethylene-glycol, diethylene glycol, 1,4-dioxane, tetrahydrofuran, 2-methoxyethanol, and 2-ethoxyethanol at 298.15 K. *J. Chem. Eng. Data,* **1995**, *40*(4), 856-861.
6. Wohlfarth, C., Dielectric constant of the mixture (1) water; (2) tetrahydrofuran. In *Static Dielectric Constants of Pure Liquids and Binary Liquid Mixtures*, Lechner, M. D., Ed. Springer: Berlin, 2008; pp 576-579.